



Association between IVIM parameters and treatment response in locally advanced squamous cell cervical cancer treated by chemoradiotherapy

Jose Angelo Udal Perucho¹ · Mandi Wang¹ · Varut Vardhanabhuti¹ · Ka Yu Tse² · Karen Kar Loen Chan² · Elaine Yuen Phin Lee¹

Received: 19 November 2020 / Revised: 7 January 2021 / Accepted: 19 February 2021 / Published online: 30 March 2021
© European Society of Radiology 2021

Abstract

Objective To examine the associations of intravoxel incoherent motion (IVIM) parameters with treatment response in cervical cancer following concurrent chemoradiotherapy (CCRT).

Materials and methods Forty-five patients, median age of 58 years (range: 28–82), with pre-CCRT and post-CCRT MRI, were retrospectively analysed. The IVIM parameters pure diffusion coefficient (D) and perfusion fraction (f) were estimated using the full b -value distribution (BVD) as well as an optimised subsample BVD. Dice similarity coefficient (DSC) and intraclass correlation coefficient (ICC) were used to measure observer repeatability in tumour delineation at both time points. Treatment response was determined by the response evaluation criteria in solid tumour (RECIST) 1.1 between MRI examinations. Mann-Whitney U tests were used to test for significant differences in IVIM parameters between treatment response groups.

Results Pre-CCRT tumour delineation repeatability was good (DSC = 0.81) while post-CCRT delineation repeatability was moderate (DSC = 0.67). Values of D and f had good repeatability at both time points (ICC > 0.80). Pre-CCRT f estimated using the full BVD and optimised subsample BVD were found to be significantly higher in patients with partial response compared to those with stable disease or disease progression ($p = 0.01$ and 95% CI = -0.02–0.00 for both cases).

Conclusion Pre-CCRT f was associated with treatment response in cervical cancer with good observer repeatability. Similar discriminative ability was also observed in estimated pre-CCRT f from an optimised subsample BVD.

Key Points

- Pre-treatment tumour delineation and IVIM parameters had good observer repeatability.
- Post-treatment tumour delineation was worse than at pre-treatment, but IVIM parameters retained good ICC.
- Pre-treatment perfusion fraction estimated from all b -values and an optimised subsample of b -values were associated with treatment response.

Keywords Uterine cervical neoplasms · Chemoradiotherapy · Observer variation · Magnetic resonance imaging · Diffusion magnetic resonance imaging

Abbreviations

ADC Apparent diffusion coefficient

✉ Elaine Yuen Phin Lee
eyplee77@hku.hk

¹ Department of Diagnostic Radiology, Queen Mary Hospital, The University of Hong Kong, Room 406, Block K, Queen Mary Hospital, Pok Fu Lam Road, Hong Kong, People's Republic of China

² Department of Obstetrics and Gynaecology, Queen Mary Hospital, The University of Hong Kong, Hong Kong, People's Republic of China

AUC	Area under the curve
BVD	B -value distribution
CCRT	Concurrent chemoradiotherapy
D	Pure diffusion coefficient
DSC	Dice similarity coefficient
D^*	Pseudo-diffusion coefficient
f	Perfusion fraction
FIGO	International Federation of Gynecology and Obstetrics
ICC	Intraclass correlation coefficient
LACC	Locally advanced cervical cancer
RECIST	Response evaluation criteria in solid tumours

MRI	Magnetic resonance imaging
ROC	Receiver operating characteristic
ROI	Region of interest
SCC	Squamous cell carcinoma
SENSE	Sensitivity encoding
TE	Echo time
TR	Repetition time
TSE	Turbo spin echo
T2W	T2-weighted
VOI	Volume of interest

Introduction

Concurrent chemoradiation (CCRT) is the recommended treatment for bulky and locally advanced cervical cancer (LACC) [1–5]. However, it has been found that 30% of patients experience treatment failure [6–8] and ultimately 40% of patients were found to have recurrence [9, 10]. Therefore, it would be beneficial to identify potential imaging biomarkers that predict patients with poor response to standard treatment for potential treatment escalation, selection for entry into clinical trials and more intensive follow-up regimen.

Quantitative evaluation of diffusion-weighted imaging (DWI) is increasingly utilised in cervical cancer due to its non-invasive nature. Previous studies have found that the apparent diffusion coefficient (ADC) was significantly different between tumour grades [11] and International Federation of Gynecology and Obstetrics (FIGO) stages [12]. ADC has also been shown to be useful in evaluating treatment response as one previous study demonstrated that baseline ADC was significantly different between patients with different overall survival [13]. Furthermore, ADC measured at baseline and in the middle of CCRT were significantly lower in patients who suffered from recurrence [14].

Previous studies showed that the diffusional signal measured in cervical cancer was better ascribed to the intravoxel incoherent motion (IVIM) phenomenon [15, 16]. This biexponential model gives rise to three parameters: the pure diffusion coefficient (D), perfusion fraction (f) and pseudo-diffusion coefficient (D^*). D aims to represent water diffusion without perfusion effects, f is a measure of the flowing blood fraction, while D^* aims to represent perfusion-related diffusion in the microcapillary network. The f and D^* were significantly different between histological subtypes of cervical cancer [17] and could monitor tumour changes during CCRT [18]. A change in D in the pelvic marrow between baseline and after CCRT could predict patients who would suffer from haematological toxicity as a result of CCRT [19].

One disadvantage of IVIM is that most acquisition protocols require more than eight b -values, leading to long

acquisition times [20, 21]. Optimised subsampling, a process which seeks to find the most important b -values for IVIM estimation, has previously been suggested to reduce the number of b -values needed. The estimated IVIM parameters from optimised subsampling had good concordance to the full acquisition estimates and retained diagnostic capabilities [22, 23]. Shorter IVIM acquisition protocol could potentially allow for clinical integration.

The purpose of this study was to evaluate the association of IVIM parameters with treatment response to CCRT in LACC and determine if an optimised subsampled IVIM had similar findings.

Materials and methods

Patients

This retrospective study was approved by the local Institutional Review Board and in accordance with the Helsinki Declaration. The study involved anonymized human data without identifying information that had already been collected waiving the need for informed consent.

Potential candidates for this retrospective study were drawn from our institute's local database. Inclusion criteria were (a) cervical carcinoma at least FIGO stage IB2 (based on FIGO 2018 revision); (b) received CCRT and subsequently intracavitary brachytherapy; and (c) had MRI examinations, once prior to treatment (pre-CCRT) and once after CCRT but before intracavitary brachytherapy (post-CCRT). Exclusion criteria were (a) poor image quality in either pre- or post-CCRT DWI; (b) prior pelvic surgery; (c) non-squamous cell carcinoma histology [24]; (d) small initial tumour volume of less than 1.5 cm³ as measured on T2-weighted (T2W) MRI; and (e) any previous history of malignant diseases apart for cervical carcinoma. All patients were restaged using the FIGO 2018 revision criteria.

Concurrent chemoradiotherapy

Patients were treated by whole-pelvic irradiation with a total cumulative dose of 40 Gy over 4 weeks with daily dose of 2Gy using 6 or 10 MV photon beams. Each week, patients also received a cycle of cisplatin (40 mg/m²).

Imaging acquisition

Patients were asked to fast for at least 6 h prior to the examination, and were given 20 mg hyoscine butylbromide (Buscopan, Boehringer) to suppress bowel peristalsis. Patients were scanned on a 3T system (Achieva 3.0T TX, Philips Healthcare). This study examined two routine clinical MRI sequences, axial and sagittal T2W, as well as DWI which

were acquired using a 16-channel phased array torso coil (Table 1). DWI was conducted in a free-breathing environment with 13 b -values [0, 10, 20, 30, 40, 50, 75, 100, 150, 300, 500, 800 and 1000 s/mm²] and had a scan time of 7 min and 16 s.

Intravoxel incoherent motion analysis

Biexponential IVIM analysis was performed using non-negative least squares (NNLS) algorithm in MATLAB (MATLAB R2020a, Mathworks Inc) according to the equation:

$$\frac{S_b}{S_0} = f e^{-b(D+D^*)} + (1-f)e^{-bD}$$

where S_b represents the mean signal intensity with diffusion gradient b , and S_0 is the mean signal intensity when $b = 0$ s/mm². Segmented fitting was used to estimate IVIM parameters which first assumed a monoexponential fit to get initial estimates of D and f and then subsequently used the initial estimates for biexponential curve fitting using a least squares estimator to refine estimates of D and f as well as estimating D^* . However, D^* was not considered for analysis in this study due to its poor reproducibility [25, 26]. The curve fitting was also constrained with $D < 3 \times 10^{-3}$ s/mm² and $f < 1$.

First, all 13 b -values were used to calculate IVIM parameters and generate parametric maps. These served as the reference parameters and hereafter referred to as the full reference b -value distribution (BVD). A recent study demonstrated that an optimal subsampled BVD using only 6 b -values could reduce scan time while retaining diagnostic capabilities [23]. Thus, 6 b -values [0, 10, 30, 75, 300, 1000 s/mm²] were then used to calculate a second set of IVIM parametric maps. This

abbreviated BVD would result in a scan time of 3 min and 18 s, representing a scan time reduction of 55%. The mean and median values of D and f were calculated from both sets of b -value distributions at both MRI examinations.

Tumour delineation

One radiologist (R1), board-certified with > 10 years' experience in abdominopelvic MRI, manually drew volumes of interest (VOIs) using the freehand selection tool on ImageJ (ImageJ 1.52a, National Institutes of Health) to encompass the whole primary tumour on T2W images $b1000$ DWI images with reference to the T2W images and D parametric maps of pre- and post-CCRT images (Fig. 1). The radiologist was given both sets of images and was aware of the sequence of the MRI examinations. The T2W VOIs were used to measure tumour volume, while the DWI VOIs were then propagated to co-registered D and f parametric maps estimated with the full BVD and optimised subsample BVD (Fig. 2). The radiologist was also asked to measure the length of the tumour's longest axis on T2W images for treatment response assessment.

To measure observer repeatability, a second radiologist (R2), with 3 years' experience in abdominopelvic MRI, delineates VOIs on pre- and post-CCRT MRI examinations as previously described. Additionally, the patient order was randomised and R1 was asked to delineate another set of VOIs on pre- and post-CCRT MRI examinations after a 1-month interval for all patients (Fig. 3).

Treatment response assessment

Patients were dichotomised by their treatment response based on the response evaluation criteria in solid tumours (RECIST) 1.1 using the longest axis measurements obtained from T2W images of the primary tumour [27]. Responders were patients with a greater than or equal to 30% reduction of the diameter of the longest axis between pre-CCRT and post-CCRT MRI examinations, or those with complete or partial response according to RECIST. Non-responders were thus patients with any of the following: a less than 30% reduction of the longest axis diameter, a 20% increment of the longest axis diameter, a new lesion, corresponding to stable or progressive disease according to RECIST.

Observer repeatability

Dice similarity coefficient (DSC), a statistic used to quantify the degree of spatial overlap between image segmentations ranging from 0 to 1 (no and complete overlap, respectively), was used to measure the degree

Table 1 Summary of MRI scan parameters

Sequences	T2W	T2W	DWI
Plane	Sagittal	Axial	Axial
Acquisition	TSE	TSE	SSEPI
TR/TE (ms)	4000/80	2800/100	2000/54
Turbo factor	30	12	NA
SENSE factor	2	2	2
Field of view (mm)	240 × 240	402 × 300	406 × 300
Matrix size	480 × 298	787 × 600	168 × 124
Slice thickness (mm)	4	4	4
Intersection gap (mm)	0	0	0
Bandwidth (Hz/pixel)	230	169	15.3
Number of excitations	2	1	2

DWI: diffusion-weighted imaging; TR/TE: repetition time/echo; TSE: turbo spin echo; SENSE: sensitivity encoding; SSEPI: single-shot echo planar imaging

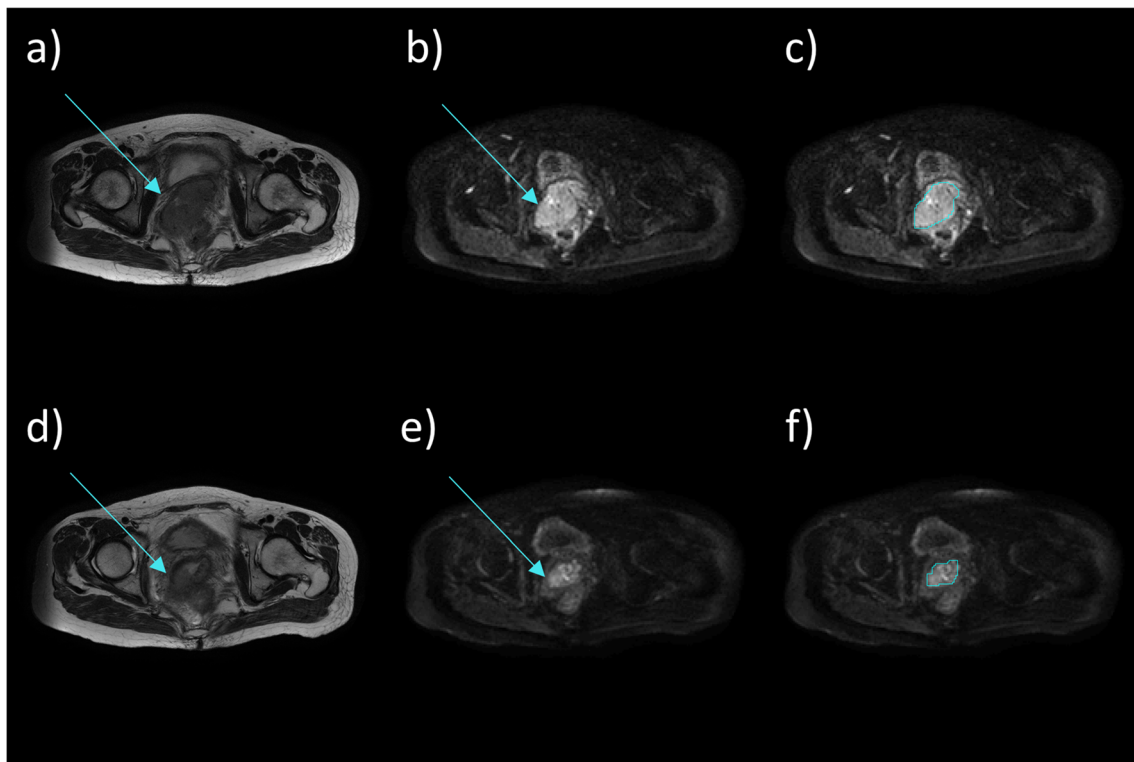


Fig. 1 Representative pre-concurrent chemoradiotherapy (pre-CCRT). **a** T2-weighted (T2W) images to aid in tumour delineation on. **b** Diffusion-weighted images (DWI), $b = 1000 \text{ s/mm}^2$. **c** Regions of interest were drawn by the senior radiologist to encompass the whole tumour area

of similarity of VOIs. A DSC of 0.70 is considered the threshold for good image segmentation repeatability [28]. Intraclass correlation coefficient (ICC) using a two-way mixed, single-score consistency model, a statistic often used to quantify the similarity of feature values, was used to measure the similarity of the calculated IVIM parameters. The feature values calculated from all three sets of VOIs were compared simultaneously to compute a single ICC value per feature. An ICC of 0.75 is considered the threshold for good measurement repeatability [29].

Statistical analysis

All statistical analyses were performed using R (R 3.6.2, R Core Team). The Fisher's exact test was used to determine if FIGO stage was associated with treatment response. Then, two-sample Mann-Whitney U tests were used to determine if there were any significant differences in MRI features between treatment response groups; the non-responder group was set to 0 while the responder group was set to 1. Finally, receiver operative characteristic (ROC) analysis was applied on significant features to compute the optimal cut-offs, area under the curve (AUC), sensitivity and specificity.

and was repeated on subsequent slices to include the entire tumour volume. The volumes of interest were propagated to co-registered pure diffusion coefficient (D) and perfusion (f) parametric maps. Tumour delineation was also done on post-CCRT images (d–f)

Results

Patient demographics

Forty-five patients from June 2014–November 2018 were included in this study (Fig. 4) and patient demographics may be found in Table 2.

Observer Repeatability

Pre-CCRT DSC was good at 0.81 while post-CCRT DSC was moderate at 0.67.

Pre- and post-CCRT ICC values were good and similar between the reference and subsampled parameters. A full tabulation of ICC values can be found in Table 3.

Associations with treatment response

Of the 45 patients, 27 had partial response, 17 had stable disease and 1 had progressive disease. None achieved complete response after CCRT. FIGO stage was not associated with treatment response ($p = 0.60$).

Pre-CCRT reference and subsampled f_{Mean} and f_{50} were observed to be significantly higher in responders compared to non-responders. No significant differences were observed

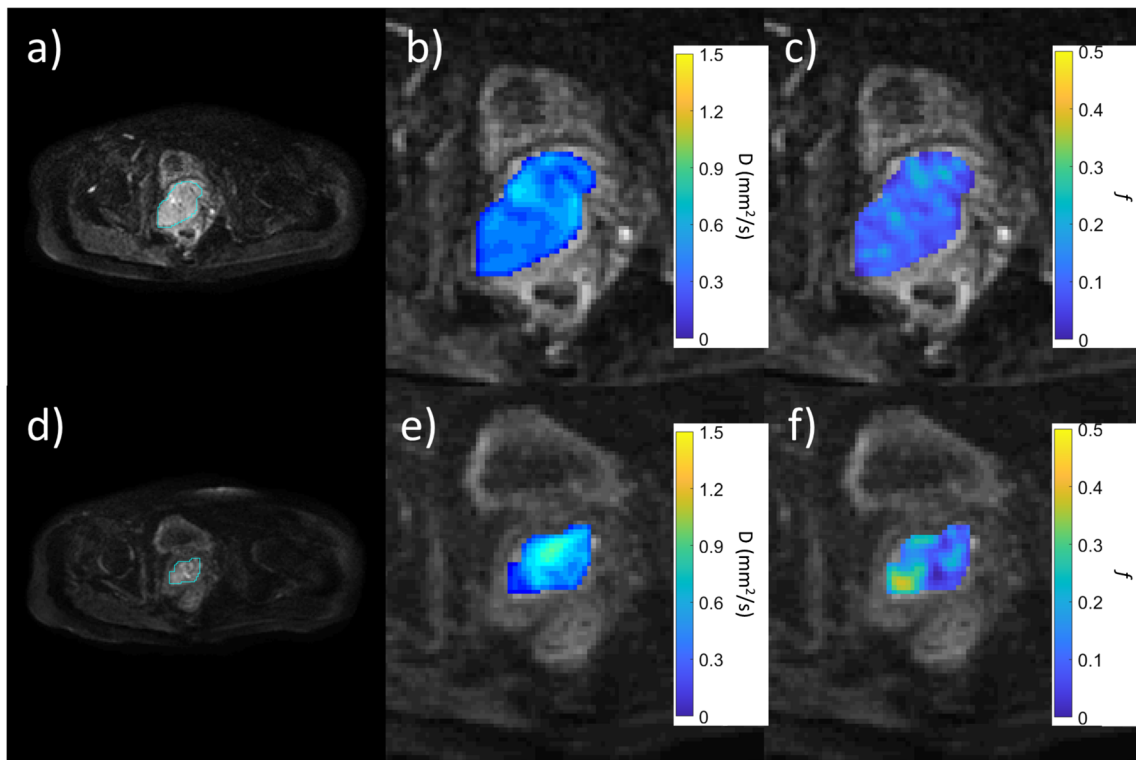
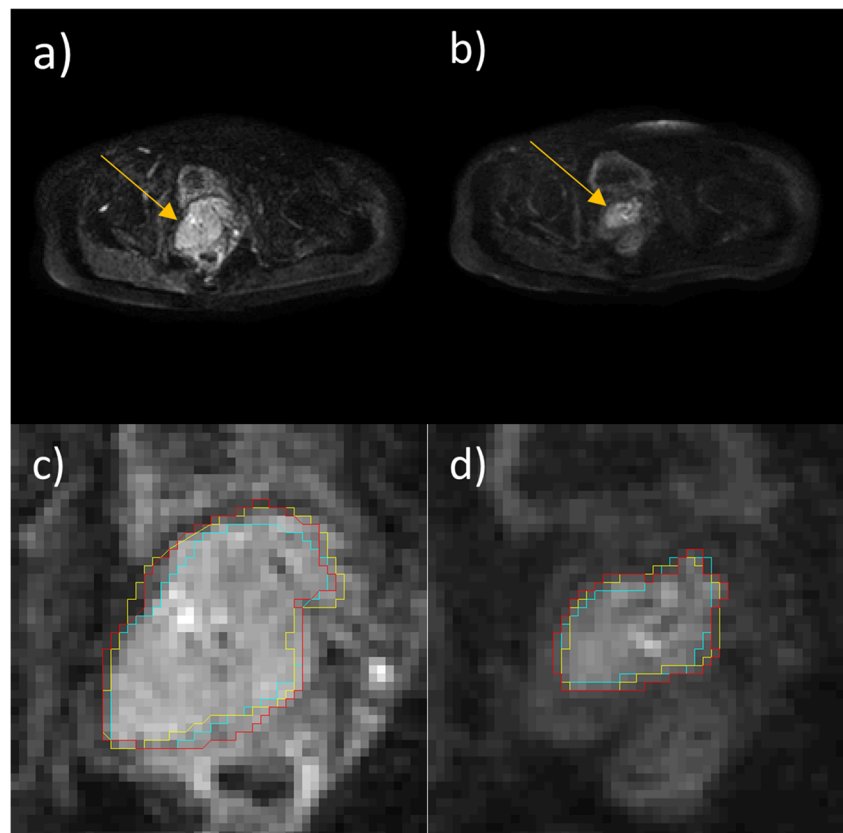


Fig. 2 Representative pre-concurrent chemoradiotherapy (pre-CCRT) **a** Diffusion-weighted images (DWI), $b = 1000 \text{ s/mm}^2$ that were also overlaid with parametric maps of **(b)** pure diffusion coefficient (D) and **(c)** perfusion fraction (f) over the tumour as well as the corresponding **(d–f)**

post-CCRT images and parametric maps. The cyan regions of interest (ROI) represent the first delineation by the senior radiologist on DWI which was copied to the D and f parametric maps

Fig. 3 Representative diffusion-weighted images (DWI) $b = 1000 \text{ s/mm}^2$ **(a)** before pre-concurrent chemoradiotherapy (pre-CCRT) and **(b)** after CCRT (post-CCRT). Regions of interest (ROIs) were drawn twice by a senior radiologist and once by a junior radiologist on both **(c)** pre-CCRT and **(d)** post-CCRT images. The segmentations by the senior radiologist are denoted by the cyan ROIs during the first reading session, and by the yellow ROIs for the second session. The delineations by the junior radiologist are denoted by red ROIs



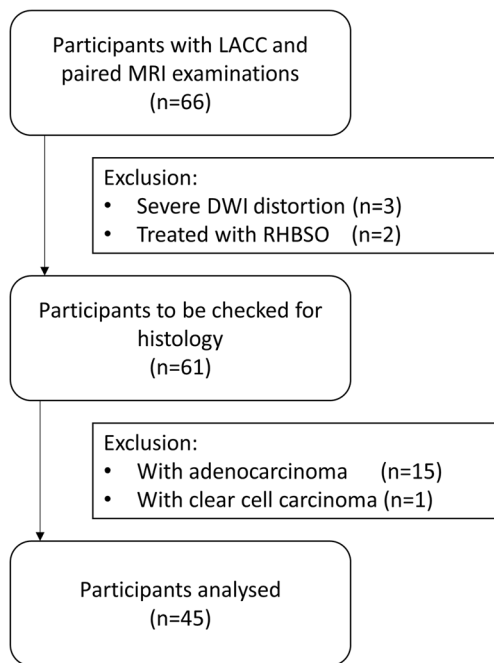


Fig. 4 Diagram of patient selection

in pre-CCRT reference and subsampled D between response groups. A full tabulation of pre-CCRT reference and subsampled parameters can be found in Table 4 and ROC performance metrics of significant features may be found on Table 5.

There were no significant differences in any post-CCRT parameters evaluated between responders and non-responders (Table 4).

Table 2 Patient characteristics

Age*	58 (28–84) years
Tumour volume*	
Pre-CCRT	44.87 (7.10–246.76) cm ³
Post-CCRT	8.08 (1.23–45.76) cm ³
FIGO stage (2018)	
IB	2
IIA	3
IIB	15
IIIB	4
IIIC	21
Grade	
1	3
2	16
3	25

CCRT: concurrent chemoradiotherapy; FIGO: International Federation of Gynecology and Obstetrics

*Value given as median and range

Discussion

In this study, we found that post-CCRT repeatability was lower than pre-CCRT in both tumour delineation and parameter value estimations. We also found that pre-CCRT f was significantly higher in responders. Furthermore, an optimal subsampled BVD estimated pre-CCRT f that had similar repeatability metrics as the full reference BVD also demonstrated the same significant difference between treatment response groups.

At baseline, we found that the DSC of tumour delineations had good agreement, which generally gave rise to good ICC in IVIM parameters. D appeared to have higher repeatability than f , which is in concordance with previous studies investigating renal tumours [30] and rectal cancer [31]. However, this is in conflict with one study investigating nasopharyngeal carcinoma that found D and f had similar repeatability [32]. It is possible that the good repeatability in D and f observed in this study may be due to volumetric delineation as a previous study found that whole-lesion VOIs had superior repeatability compared to single-slice regions of interest (ROIs) [33]. After treatment, we found that the DSC of tumour delineations was only moderate; despite this, the ICC of reference and subsampled post-CCRT D and f remained good. Post-CCRT assessment of cervical cancer is known to be challenging due to a host of irradiative changes and could be a reason for the lowered repeatability of post-CCRT tumour delineations and IVIM parameter values [34, 35]. The smaller tumour volumes presented on post-CCRT scans may be another contributing factor as there are fewer pixels to average IVIM parameter values over [36].

Values of D were not significantly different between treatment response groups at either time point. Similar studies have found that pre-CCRT ADC and D had limited value in predicting short- and long-term treatment response, though mid-treatment ADC was shown to have some prognostic value [37–40]. However, this is in contrast to a recent study that demonstrated pre-CCRT D was significantly lower in responders [41].

In this study, we found that pre-CCRT f was significantly higher in responders compared to non-responders. A previous cervical cancer study had similar findings, where the authors found that f was significantly higher in patients with complete response compared to those with partial response [42]. Furthermore, in a study examining long-term prognosis, higher post-CCRT f has been shown to be able to predict good prognosis in cervical cancer [39]. Given the significant correlations between IVIM and dynamic contrast-enhanced (DCE)-MRI parameters [43], our result concurred with DCE-MRI in that better perfused tumours had better locoregional control [44–46]. Elevated pre-treatment perfusion on MRI suggests better oxygenated tumours [47], a determinant of better locoregional control and also improved disease-free and overall survival [48]. It is thought that hypoxia induced genetic instability that leads to increased radioresistance in tumours

Table 3 Values and intraclass correlation coefficient (ICC) of pure diffusion coefficient (D) and perfusion fraction (f) before concurrent chemoradiotherapy (pre-CCRT) and after treatment (post-CCRT) derived from the full reference b -value distribution (BVD) and subsampled BVD, and from the different observers. R1-1 and R2-1 correspond to the IVIM parameters as estimated from the first set of volumes of interest (VOIs) from the first and second radiologist, respectively, while R1-2 corresponds to the parameters estimated from the second set of VOIs of the first radiologist

Features		Pre-CCRT		Post-CCRT	
		Reference	Subsampled	Reference	Subsampled
$D_{50}†$	R1-1	0.78 (0.58–0.97)	0.78 (0.58–0.97)	1.09 (0.84–1.42)	1.09 (0.84–1.43)
	R1-2	0.82 (0.64–0.98)	0.82 (0.64–0.98)	1.06 (0.82–1.40)	1.07 (0.79–1.40)
	R2-1	0.79 (0.61–0.97)	0.79 (0.61–0.97)	1.06 (0.79–1.40)	1.07 (0.79–1.40)
	ICC	0.96	0.96	0.82	0.89
$D_{Mean}†$	R1-1	0.81 (0.60–0.98)	0.81 (0.61–0.98)	1.10 (0.85–1.40)	1.10 (0.82–1.40)
	R1-2	0.86 (0.69–0.99)	0.86 (0.69–0.99)	1.08 (0.80–1.36)	1.08 (0.76–1.36)
	R2-1	0.82 (0.65–1.09)	0.82 (0.62–1.02)	1.07 (0.81–1.37)	1.07 (0.80–1.38)
	ICC	0.87	0.89	0.84	0.86
f_{50}	R1-1	0.10 (0.08–0.16)	0.11 (0.08–0.16)	0.17 (0.10–0.27)	0.17 (0.10–0.30)
	R1-2	0.12 (0.08–0.15)	0.12 (0.09–0.16)	0.17 (0.11–0.27)	0.17 (0.11–0.32)
	R2-1	0.11 (0.08–0.15)	0.11 (0.08–0.15)	0.16 (0.09–0.23)	0.17 (0.08–0.29)
	ICC	0.90	0.82	0.80	0.80
f_{Mean}	R1-1	0.13 (0.11–0.18)	0.13 (0.10–0.18)	0.19 (0.12–0.28)	0.19 (0.11–0.31)
	R1-2	0.15 (0.11–0.20)	0.15 (0.11–0.19)	0.19 (0.13–0.27)	0.19 (0.11–0.32)
	R2-1	0.13 (0.10–0.18)	0.13 (0.10–0.17)	0.18 (0.11–0.26)	0.18 (0.10–0.31)
	ICC	0.79	0.78	0.79	0.81

Values expressed as median (range)

†in units of $\times 10^{-3}$ s/mm²

Table 4 Pure diffusion coefficient (D) and perfusion fraction (f) before and after concurrent chemoradiotherapy (pre-CCRT and post-CCRT, respectively) dichotomised by treatment response groups using the full 13 b -value distribution (BVD) and using an optimised subsample of 6 b -values. Responders were defined as patients whose tumour had at least 30% reduction in long axis diameter between MRI examinations

	Full BVD				Subsampled BVD			
	Non-responders	Responders	p	95% CI	Non-responders	Responders	p	95% CI
Pre-CCRT								
$D_{50}†$	0.75 (0.62–0.95)	0.81 (0.58–0.99)	0.12	(-0.11–0.02)	0.75 (0.62–0.95)	0.81 (0.58–1.00)	0.14	(-0.11–0.02)
$D_{Mean}†$	0.77 (0.66–0.96)	0.82 (0.60–1.06)	0.16	(-0.11–0.02)	0.77 (0.66–0.96)	0.82 (0.61–1.06)	0.18	(-0.11–0.02)
f_{50}	0.10 (0.08–0.15)	0.11 (0.08–0.16)	0.01*	(-0.02–0.00)	0.10 (0.08–0.16)	0.12 (0.09–0.16)	0.01*	(-0.02–0.00)
f_{Mean}	0.12 (0.11–0.18)	0.14 (0.11–0.17)	0.02*	(-0.02–0.00)	0.12 (0.10–0.18)	0.14 (0.11–0.18)	0.02*	(-0.03–0.00)
Post-CCRT								
$D_{50}†$	1.08 (0.84–1.22)	1.11 (0.86–1.42)	0.12	(-0.18–0.01)	1.07 (0.84–1.22)	1.11 (0.86–1.43)	0.10	(-0.18–0.01)
$D_{Mean}†$	1.09 (0.85–1.24)	1.10 (0.93–1.39)	0.09	(-0.19–0.02)	1.08 (0.82–1.24)	1.11 (0.94–1.39)	0.08	(-0.20–0.01)
f_{50}	0.17 (0.10–0.25)	0.17 (0.11–0.27)	0.74	(-0.03–0.02)	0.17 (0.10–0.30)	0.18 (0.12–0.27)	0.40	(-0.03–0.02)
f_{Mean}	0.19 (0.12–0.28)	0.19 (0.13–0.28)	0.85	(-0.03–0.02)	0.19 (0.11–0.31)	0.19 (0.14–0.28)	0.86	(-0.04–0.02)
Percent difference (%)								
$D_{50}†$	31.2 (11.2–87.3)	33.4 (-0.6–103.3)	0.50	(-16–8.9)	32.4 (12.8–83.3)	34.1 (-0.6–103.9)	0.44	(-17.0–9.0)
$D_{Mean}†$	29.6 (6.5–70.3)	33.3 (4.1–95.5)	0.53	(-15.3–8.8)	30.5 (7.2–66.6)	33.9 (4.5–95.4)	0.51	(-16.3–9.3)
f_{50}	67.1 (6.3–189.4)	49.9 (-10.5–126.1)	0.34	(-11.8–37.8)	63.3 (13.4–227)	51.8 (-8.3–138.8)	0.51	(-13.2–32.2)
f_{Mean}	49 (10.4–137.8)	39.7 (4.7–99.8)	0.28	(-9.4–25.6)	50.7 (-6.1–163.8)	45.6 (-1.2–96.4)	0.38	(-10–26.3)

Values expressed as median (range)

CI: confidence interval

†in units of $\times 10^{-3}$ s/mm²

* $p < 0.05$

Table 5 Receiver operating characteristic (ROC) curve performance metrics of the mean and 50th percentile of perfusion coefficient (f) before concurrent chemoradiotherapy (pre-CCRT) using the full 13 b -value distribution (BVD) and using an optimised subsample of 6 b -values

Feature	Cut-off	AUC	Sensitivity	Specificity
Full BVD				
f_{50}	0.09	0.73	0.86	0.64
f_{Mean}	0.12	0.71	0.78	0.67
Subsampled BVD				
f_{50}	0.10	0.73	0.70	0.78
f_{Mean}	0.12	0.71	0.85	0.56

AUC: area under the curves

and, thus, poor prognosis for tumours with low oxygenation measurements [49].

One limiting factor of IVIM is the long scan time due to the acquisition of substantially more b -values compared to conventional DWI. This study also examined the utility of an optimised subsampled BVD, which could potentially reduce the scan time needed for IVIM imaging. In terms of repeatability, the pre-CCRT ICC of the subsampled D and f were similar to those of reference D and f . This was in contrast with a previous study in renal tumours which found that the repeatability metrics of an abbreviated IVIM sequence was lower than a longer acquisition sequence [30]. However, in that study, the abbreviated IVIM sequence used a lower maximal b -value compared to the longer IVIM sequence which may have adversely affected parameter estimation in the abbreviated IVIM sequence [23]. Post-CCRT ICC of subsampled D was also comparable to that of reference D ; however, interestingly, post-CCRT ICC of subsampled f was good while those of reference f were only moderate. Encouragingly, similar to pre-CCRT reference f , we found that pre-CCRT subsampled f was also significantly higher in responders compared to non-responders. This implies that subsampled parameters had similar discriminative abilities as the reference parameters while only requiring half the acquisition time.

There are several limitations in this study. Firstly, VOI segmentation was done manually. Fully or semi-automatic segmentation is means to improve delineation consistency; however, there are substantial challenges to these approaches in MRI due to the heterogeneity in acquisition parameters and sequences used [50]. Secondly, this study only included a relatively small set of patients from a single centre. However, all patients had the same treatment regimen and schedule and imaging protocol. Third, scan-rescan reproducibility could not be evaluated as this was a retrospective study. Additionally, other prognostic factors such as nodal status, lymphovascular invasion and parametrial involvement to predict treatment response

were not considered; future studies combining other prognostic factors with IVIM-based features into a multivariable model could be of interest in improving the prediction of treatment response.

In conclusion, pre-CCRT f was significantly higher in responders compared to non-responders and had good observer repeatability. Furthermore, f estimated using an optimised subsampled BVD demonstrated the same association with treatment response and repeatability metrics as f estimated using the full reference BVD.

Funding This study has received funding by the General Research Fund (GRF, No. 17119916) of the Research Grants Council (RGC), Hong Kong.

Declarations

Guarantor The scientific guarantor of this publication is Dr. Elaine Y.P. Lee.

Conflict of interest The authors of this manuscript declare no relationships with any companies whose products or services may be related to the subject matter of the article.

Statistics and biometry No complex statistical methods were necessary for this paper.

Informed consent Written informed consent was waived by the Institutional Review Board.

Ethical approval Institutional Review Board of the University of Hong Kong/Hospital Authority Hong Kong West Cluster (Reference No. UW 16-325) approval was obtained.

Study subjects or cohorts overlap Some study subjects or cohorts have been previously reported on in previous studies with different aims than the current manuscript.

One study in *Journal of Magnetic Resonance Imaging* investigated the relationship between intravoxel incoherent motion (IVIM) and dynamic contrast-enhanced (DCE) MRI in cervical cancer perfusion.

One study in *Korean Journal of Radiology* assessed the feasibility of a parameter-free IVIM approach in locally advanced cervical cancer to determine the optimal b -value threshold for different histological cancer types.

One study in *Acta Radiologica Open* examined the associations of texture features of T2W and DWI with tumour histological grading and pelvic lymph nodal status.

One study in *Journal of Magnetic Resonance Imaging* investigated the bone marrow changes after concurrent chemoradiotherapy (CCRT) using IVIM and correlated these parameters with haematological toxicity in patients with cervical cancer.

One study in *BMC Cancer* assessed the concordance between the metabolic tumour volume measured by positron emission tomography (PET), anatomical tumour volume measured by T2-weighted (T2W) MRI and the functional tumour volume measured on diffusion-weighted MRI in cervical cancer.

One study in *Academic Radiology* examined the utility of diffusion kurtosis imaging in the characterisation of cervical cancer.

One study in *Korean Journal of Radiology* aimed to optimise the number of b -values needed for IVIM analysis in cervical cancer using simulated and in vivo data.

One study in *European Radiology* investigated the associations of histogram features of T2W and apparent diffusion coefficient (ADC) with treatment response of cervical cancer following CCRT

Methodology

- retrospective
- observational
- performed at one institution

References

1. Keys HM, Bundy BN, Stehman FB et al (1999) Cisplatin, radiation, and adjuvant hysterectomy compared with radiation and adjuvant hysterectomy for bulky stage IB cervical carcinoma. *N Engl J Med* 340:1154–1161
2. Morris M, Eifel PJ, Lu J et al (1999) Pelvic radiation with concurrent chemotherapy compared with pelvic and para-aortic radiation for high-risk cervical cancer. *N Engl J Med* 340:1137–1143
3. Rose PG, Bundy BN, Watkins EB et al (1999) Concurrent cisplatin-based radiotherapy and chemotherapy for locally advanced cervical cancer. *N Engl J Med* 340:1144–1153
4. Whitney CW, Sause W, Bundy BN et al (1999) Randomized comparison of fluorouracil plus cisplatin versus hydroxyurea as an adjunct to radiation therapy in stage IIB-IVA carcinoma of the cervix with negative para-aortic lymph nodes: a gynecologic oncology group and southwest oncology group study. *J Clin Oncol* 17:1339–1348
5. Peters W III (1999) Cisplatin and 5-fluorouracil plus radiation therapy are superior to radiation therapy as adjunctive in high-risk early stage carcinoma of the cervix after radical hysterectomy and pelvic lymphadenectomy: report of a phase III intergroup study. *Gynecol Oncol* 72:443
6. Collaboration CCRCCM-A (2008) Reducing uncertainties about the effects of chemoradiotherapy for cervical cancer: a systematic review and meta-analysis of individual patient data from 18 randomized trials. *J Clin Oncol* 26:5802–5812
7. Boers A, Arts HJ, Klip H et al (2014) Radical surgery in patients with residual disease after (chemo) radiation for cervical cancer. *Int J Gynecol Cancer* 24:1276–1285
8. Su T-P, Lin G, Huang Y-T et al (2018) Comparison of positron emission tomography/computed tomography and magnetic resonance imaging for posttherapy evaluation in patients with advanced cervical cancer receiving definitive concurrent chemoradiotherapy. *Eur J Nucl Med Mol Imaging* 45:727–734
9. Kirwan JM, Symonds P, Green JA, Tierney J, Collingwood M, Williams CJ (2003) A systematic review of acute and late toxicity of concomitant chemoradiation for cervical cancer. *Radiother Oncol* 68:217–226
10. Markman M (2013) Chemoradiation in the management of cervix cancer: current status and future directions. *Oncology* 84:246–250
11. Downey K, Riches SF, Morgan VA et al (2013) Relationship between imaging biomarkers of stage I cervical cancer and poor-prognosis histologic features: quantitative histogram analysis of diffusion-weighted MR images. *AJR Am J Roentgenol* 200:314–320
12. McVeigh PZ, Syed AM, Milosevic M, Fyles A, Haider MA (2008) Diffusion-weighted MRI in cervical cancer. *Eur Radiol* 18:1058–1064
13. Ueno Y, Lisbona R, Tamada T, Alaref A, Sugimura K, Reinhold C (2017) Comparison of FDG PET metabolic tumour volume versus ADC histogram: prognostic value of tumour treatment response and survival in patients with locally advanced uterine cervical cancer. *Br J Radiol* 90:20170035
14. Meng J, Zhu L, Zhu L et al (2017) Whole-lesion ADC histogram and texture analysis in predicting recurrence of cervical cancer treated with CCRT. *Oncotarget* 8:92442
15. Lee EY, Yu X, Chu MM et al (2014) Perfusion and diffusion characteristics of cervical cancer based on intravoxel incoherent motion MR imaging—a pilot study. *Eur Radiol* 24:1506–1513
16. Le Bihan D, Breton E, Lallemand D, Aubin ML, Vignaud J, Laval-Jeantet M (1988) Separation of diffusion and perfusion in intravoxel incoherent motion MR imaging. *Radiology* 168:497–505
17. Winfield JM, Orton MR, Collins DJ et al (2017) Separation of type and grade in cervical tumours using non-mono-exponential models of diffusion-weighted MRI. *Eur Radiol* 27:627–636
18. Zhu L, Zhu L, Shi H et al (2016) Evaluating early response of cervical cancer under concurrent chemo-radiotherapy by intravoxel incoherent motion MR imaging. *BMC Cancer* 16:79
19. Lee EYP, Perucho JAU, Vardhanabhuti V et al (2017) Intravoxel incoherent motion MRI assessment of chemoradiation-induced pelvic bone marrow changes in cervical cancer and correlation with hematological toxicity. *J Magn Reson Imaging* 46:1491–1498
20. Lemke A, Stieltjes B, Schad LR, Laun FB (2011) Toward an optimal distribution of b values for intravoxel incoherent motion imaging. *Magn Reson Imaging* 29:766–776
21. Ivan J, Harri M, Aronen HJ et al (2014) Optimization of b-value distribution for biexponential diffusion-weighted MR imaging of normal prostate. *J Magn Reson Imaging* 39:1213–1222
22. Dyvorne H, Jajamovich G, Kakite S, Kuehn B, Taouli B (2014) Intravoxel incoherent motion diffusion imaging of the liver: optimal b-value subsampling and impact on parameter precision and reproducibility. *Eur J Radiol* 83:2109–2113
23. Perucho JAU, Chang HCC, Vardhanabhuti V et al (2020) B-value optimization in the estimation of intravoxel incoherent motion parameters in patients with cervical cancer. *Korean J Radiol* 21:218–227
24. Hu K, Wang W, Liu X, Meng Q, Zhang F (2018) Comparison of treatment outcomes between squamous cell carcinoma and adenocarcinoma of cervix after definitive radiotherapy or concurrent chemoradiotherapy. *Radiat Oncol* 13:249
25. Andreou A, Koh DM, Collins DJ et al (2013) Measurement reproducibility of perfusion fraction and pseudodiffusion coefficient derived by intravoxel incoherent motion diffusion-weighted MR imaging in normal liver and metastases. *Eur Radiol* 23:428–434
26. Winfield JM, deSouza NM, Priest AN et al (2015) Modelling DW-MRI data from primary and metastatic ovarian tumours. *Eur Radiol* 25:2033–2040
27. Fournier L, Ammari S, Thiam R, Cuénod CA (2014) Imaging criteria for assessing tumour response: RECIST, mRECIST, Cheson. *Diagn Interv Imaging* 95:689–703
28. Zijdenbos AP, Dawant BM, Margolin RA, Palmer AC (1994) Morphometric analysis of white matter lesions in MR images: method and validation. *IEEE Trans Med Imaging* 13:716–724
29. Koo TK, Li MY (2016) A guideline of selecting and reporting intraclass correlation coefficients for reliability research. *J Chiropr Med* 15:155–163
30. Pan J, Zhang H, Man F et al (2018) Measurement and scan reproducibility of parameters of intravoxel incoherent motion in renal tumor and normal renal parenchyma: a preliminary research at 3.0 T MR. *Abdom Radiol (NY)* 43:1739–1748
31. Sun H, Xu Y, Xu Q, Shi K, Wang W (2017) Rectal cancer: short-term reproducibility of intravoxel incoherent motion parameters in 3.0T magnetic resonance imaging. *Medicine (Baltimore)* 96:e6866
32. Chen WB, Zhang B, Liang L, Dong YH, Cai GH, Liang CH, Lan BW, Zhang SX (2017) To predict the radio sensitivity of nasopharyngeal carcinoma using intravoxel incoherent motion MRI at 3.0 T. *Oncotarget* 8(32):53740–53750

33. Song M, Yue Y, Jin Y et al (2020) Intravoxel incoherent motion and ADC measurements for differentiating benign from malignant thyroid nodules: utilizing the most repeatable region of interest delineation at 3.0 T. *Cancer Imaging* 20:9
34. Papadopoulou I, Stewart V, Barwick TD et al (2016) Post–radiation therapy imaging appearances in cervical carcinoma. *Radiographics* 36:538–553
35. Addley HC, Vargas HA, Moyle PL, Crawford R, Sala E (2010) Pelvic imaging following chemotherapy and radiation therapy for gynecologic malignancies. *Radiographics* 30:1843–1856
36. Pathak R, Ragheb H, Thacker NA et al (2017) A data-driven statistical model that estimates measurement uncertainty improves interpretation of ADC reproducibility: a multi-site study of liver metastases. *Sci Rep* 7:1–10
37. Meng J, Liu S, Zhu L et al (2018) Texture analysis as imaging biomarker for recurrence in advanced cervical cancer treated with CCRT. *Sci Rep* 8:11399
38. Meng J, Zhu L, Zhu L et al (2017) Histogram analysis of apparent diffusion coefficient for monitoring early response in patients with advanced cervical cancers undergoing concurrent chemo-radiotherapy. *Acta Radiol* 58:1400–1408
39. Zhu L, Wang H, Zhu L et al (2017) Predictive and prognostic value of intravoxel incoherent motion (IVIM) MR imaging in patients with advanced cervical cancers undergoing concurrent chemo-radiotherapy. *Sci Rep* 7:11635
40. Bowen SR, Yuh WT, Hippe DS et al (2018) Tumor radiomic heterogeneity: multiparametric functional imaging to characterize variability and predict response following cervical cancer radiation therapy. *J Magn Reson Imaging* 47:1388–1396
41. Zhang H, Zhou Y, Li J, Zhang P, Li Z, Guo J (2020) The value of DWI in predicting the response to synchronous radiochemotherapy for advanced cervical carcinoma: comparison among three mathematical models. *Cancer Imaging* 20:8
42. Zhu L, Zhu L, Wang H et al (2017) Predicting and early monitoring treatment efficiency of cervical cancer under concurrent chemoradiotherapy by intravoxel incoherent motion magnetic resonance imaging. *J Comput Assist Tomogr* 41:422–429
43. Lee EY, Hui ES, Chan KK et al (2015) Relationship between intravoxel incoherent motion diffusion-weighted MRI and dynamic contrast-enhanced MRI in tissue perfusion of cervical cancers. *J Magn Reson Imaging* 42:454–459
44. Loncaster JA, Carrington BM, Sykes JR et al (2002) Prediction of radiotherapy outcome using dynamic contrast enhanced MRI of carcinoma of the cervix. *Int J Radiat Oncol Biol Phys* 54:759–767
45. Mayr NA, Yuh WT, Magnotta VA et al (1996) Tumor perfusion studies using fast magnetic resonance imaging technique in advanced cervical cancer: a new noninvasive predictive assay. *Int J Radiat Oncol Biol Phys* 36:623–633
46. Gong QY, Brunt JN, Romaniuk CS et al (1999) Contrast enhanced dynamic MRI of cervical carcinoma during radiotherapy: early prediction of tumour regression rate. *Br J Radiol* 72:1177–1184
47. Zahra MA, Hollingsworth KG, Sala E, Lomas DJ, Tan LT (2007) Dynamic contrast-enhanced MRI as a predictor of tumour response to radiotherapy. *Lancet Oncol* 8:63–74
48. Lyng H, SundfØr K, Tropé C, Rofstad EK (2000) Disease control of uterine cervical cancer: relationships to tumor oxygen tension, vascular density, cell density, and frequency of mitosis and apoptosis measured before treatment and during radiotherapy. *Clin Cancer Res* 6:1104–1112
49. Hall EJ, Giaccia AJ (2006) *Radiobiology for the radiologist*. Lippincott Williams & Wilkins
50. Lenchik L, Heacock L, Weaver AA et al (2019) Automated segmentation of tissues using CT and MRI: a systematic review. *Acad Radiol* 26:1695–1706

Publisher's note Springer Nature remains neutral with regard to jurisdictional claims in published maps and institutional affiliations.